# Quantitative Measurement of Dispersion of Carbon Black in Rubber by an Image Processing Technique

L. GANESAN,[1] PRITIMOY BHATTACHARYYA,[1] and ANIL K. BHOWMICK[2,*]

[1]Department of Computer Science and Engineering and [2]Rubber Technology Center, Indian Institute of Technology, Kharagpur - 721 302, India

## SYNOPSIS

In this article, the quantification of dispersion of carbon black in rubber is done by an image-processing technique. Surfaces, having different dispersion ratings, are mostly textured. These textured surfaces are digitized and the images are analyzed for quantification. Textured images are suitably represented by a closed set of orthogonal polynomials. The presence of texture has been identified by suitably measuring the orthogonal effects. The textured surfaces are described locally by pronum and globally by prospectrum. Mean, variance, and Fisher distance were computed from the prospectrums and are correlated to various dispersion ratings. There is a linear relationship between the calculated mean and the dispersion rating. © 1995 John Wiley & Sons, Inc.

## INTRODUCTION

The properties of rubber products containing reinforcing fillers or pigments is highly dependent on uniform dispersion of these ingredients in rubber. For example, poor dispersion would lead to reduced product life or poor performance during service, poor product appearance, poor processing and manufacturing uniformity, waste of raw materials, and excessive energy usage. Therefore, considerable time and effort of a large number of workers have been devoted to developing suitable test procedures for the characterization of dispersion. Hess[1] recently reviewed the subject. The methods available are optical microscopy, X-ray radiography, transmission electron micrography, surface inspection, stylus surface measurement, optical scanning of surfaces, electrical conductivity, pyrolysis gas chromatography, etc. All these methods suffer from one or more limitations, especially in quantification of dispersion, although attempts have been made to do so by using the comparatively easier techniques. For example, Medalia[2] prepared a dispersion chart using carbon black at different percentage levels of dispersion. This chart is made up of 48 optical micrographs. However, quantitative analysis of optical, TEM, and SEM images using on line or off-line image analyzers is possible. Multiple features in the images are analyzed simultaneously for different parameters like area, perimeters, etc.[3] Hess[1] pointed out that these measurements have been more directly related to characterizing morphology of carbon black than has dispersion. Shih and Goldfinger[4] and Kadunce[5] recently reported success in the image analysis. However, the present authors feel that there is a further scope of statistical analysis of the images using a computer in order to interpret the dispersion correctly and quickly. It is with this objective that we have applied our recent techniques of pattern recognition to analyze the dispersion of carbon black in rubber. Ganesan and Bhattacharyya[6] analyzed various types of textured images on the basis of a closed set of orthogonal polynomials. Haralick,[7] Galloway,[8] and He and Wang[9] also reported various texture analysis schemes.

## PROPOSED MODEL FOR TEXTURE ANALYSIS

Texture is defined as a structure composed of a large number of more or less ordered, similar elements or

* To whom correspondence should be addressed.

Journal of Applied Polymer Science, Vol. 56, 1739–1747 (1995)
 CCC 0021-8995/95/131739-09

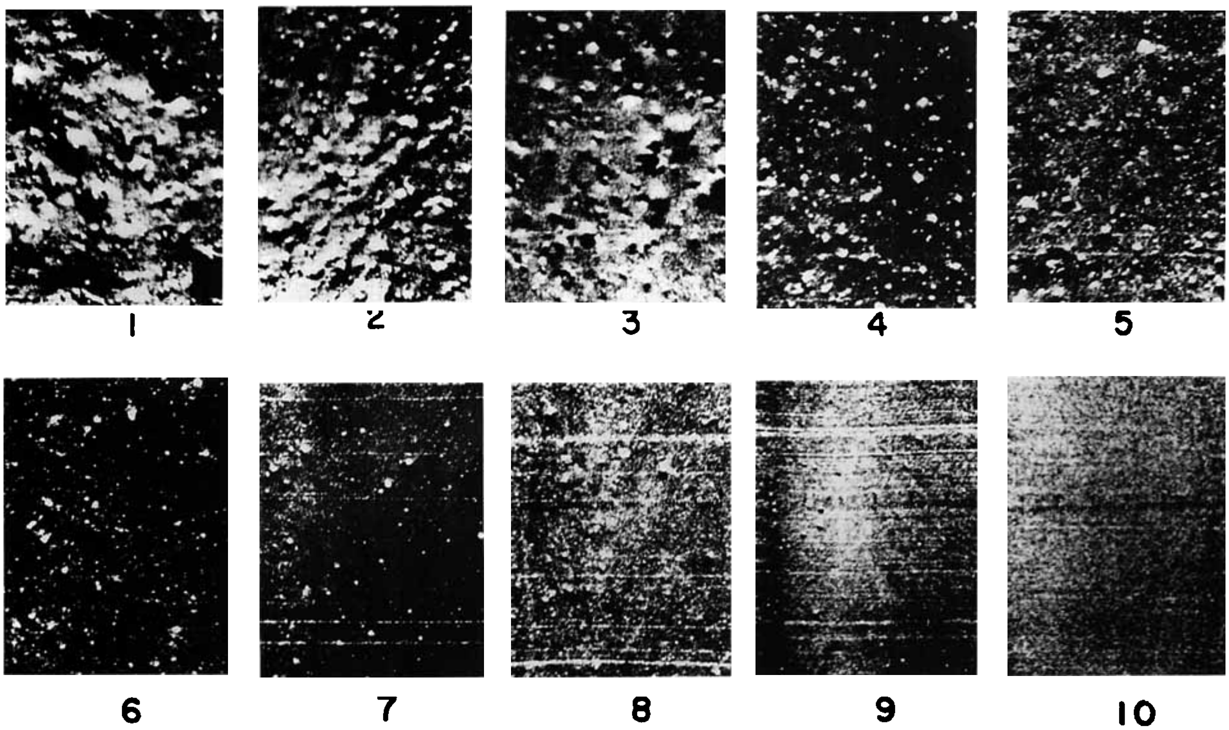

**Figure 1** Various images having dispersion rating from very poor to excellent.

primitives. Textures are normally ranging from micro to macro. A microtexture appears only in a small area of digital image with very high gray-level variations, i.e., significant tonal variation within a small image region. Microtextures can be studied effectively by using local properties. The quantified local property of a microtexture is called the local descriptor for the texture or pronum. The whole textured image can be represented globally by computing the frequency of occurrences of pronums. This frequency of occurrences of pronums will be called prospectrum. The prospectrum is unique for a textured image.

## Texture Detection

Consider an $(N * N)$ gray-level image $f(x, y)$, where $x$ and $y$ are the two Cartesian coordinates. $f(x, y)$ can be expressed as

$$f(x, y) = g(x, y) + \eta(x, y) \tag{1}$$

where $g(x, y)$ accounts for the variation in Cartesian coordinates resulting in texture and $\eta(x, y)$ is the additive noise.

To measure the variations resulting from texture and noise separately, we represent $f(x, y)$ as follows in terms of a set of uncorrelated basis variations[10] in Cartesian coordinates:

$$[f_{i,j}^N] = \sum_{i=0}^{N-1} \sum_{j=0}^{N-1} \beta_{ij}[O_{i,j}^N] \tag{2}$$

where $[f_{i,j}^N]$ is the $(N * N)$ gray-level image matrix, $[O_{i,j}^N]$ accounts for the model variation in coordinates, and $\beta_{ij}$ is the $(i, j)$th coefficient of variation. $\beta_{ij}$ is basically the effect of the variation accounted for by $[O_{i,j}^N]$ over the image region $f(x, y)$. We select $[O_{i,j}^N]$'s in such a manner that these are orthogonal to each other to separate the two variables. These variations due to Cartesian coordinates are categorized into two groups. In one, both the coordinates vary jointly. In the other, one coordinate at a time is varying when the other remains constant. The orthogonal effects due to the first type of variation are called the interaction effects, whereas the orthogonal effects due to the second type of variation are called the main effects. It has been observed experimentally[6] that the variation in Cartesian coordinates that causes the interaction effects results

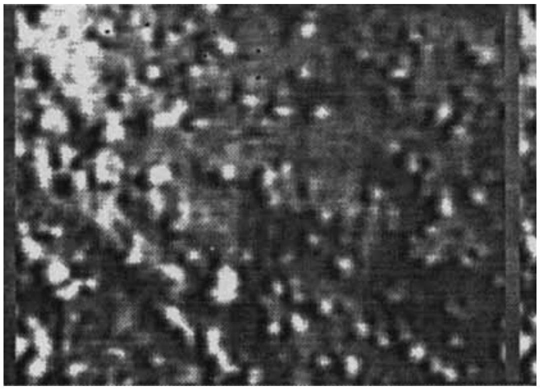

1–2

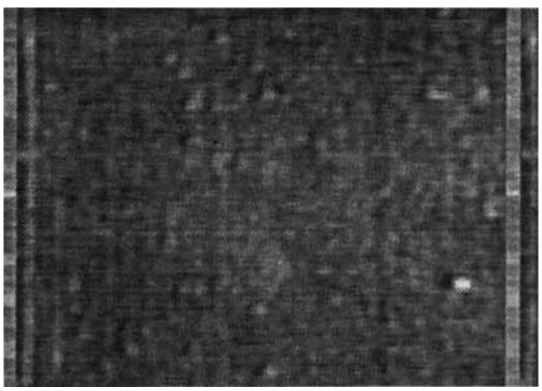

1–8

**Figure 2** Digitized version of the images shown in Figure 1-2, and 1-8.

from textures. Hence, the texture is characterized by the interaction effects. For computing orthogonal effects, we propose a set of orthogonal polynomials $\phi_0(x), \phi_1(x), \ldots, \phi_N(x)$, the generating formula of which is given in Ref. 6. Using these orthogonal polynomials, eq. (1) can be written as

$$f(x, y) = \sum \sum_{\beta_{ij} \in \text{ set of interaction effects}} \beta_{ij}\phi_i(x)\phi_j(y) + \sum \sum_{\beta_{ij} \in \text{ set of main effects}} \beta_{ij}\phi_i(x)\phi_j(y) \quad (3)$$

We call $\beta_{ij}$ and $\beta_{ij}^2 \langle \phi_i, \phi_i \rangle \langle \phi_j, \phi_j \rangle$, respectively, the estimates of the orthogonal effect and the corresponding mean square variance. Equation (2) can be written in matrix notation as follows:

$$[f_{ij}^N] = \sum_{i=0}^{N-1} \sum_{j=0}^{N-1} \beta_{ij}\hat{P}_i\hat{P}_j^t \quad (4)$$

where $\hat{P}_i$ is a column vector of size $(N * 1)$ consisting of values of the polynomials $\phi_i(x)$ at $x = x_1 = 1$, $x = x_2 = 2, \ldots, x = x_N = N$ and $\hat{P}_j^t$ is the transpose of the column vector $\hat{P}_j$ of size $(N * 1)$. $\hat{P}_j$ consists of values of the polynomial $\phi_j(y)$ at $y = y_1 = 1$, $y = y_2 = 2, \ldots, y = y_N = N$. The orthogonal effects can be computed as

$$[\beta_{ij}] = ([M]^t[M])^{-1}([M]^t[f][M])([M]^t[M])^{-1} \quad (5)$$

where $[M]$ is a matrix of size $(N * N)$. $[M]$ is obtained as follows:

$$[M] = [\hat{P}_0, \hat{P}_1, \ldots, \hat{P}_{N-1}]$$

From eq. (5), the main effects resulting in noise are given by

$$\beta_{\mathbf{ij}}^{\mathbf{1}} = \{\beta_{\mathbf{ij}}: \quad \mathbf{0 < i + j \le 2}, \quad \mathbf{i \ne j}\} \quad (6)$$

and the interaction effects characterizing the texture are

$$\beta_{\mathbf{ij}}^{\mathbf{2}} = \{\beta_{\mathbf{ij}}: \quad \mathbf{0 < i, j < 3}\} \quad (7)$$

The mean squares corresponding to the orthogonal effects can be computed as

$$[Z_{ij}^2] = ([M]^t[M])^{-1}([M]^t[f][M])^2([M]^t[M])^{-1} \quad (8)$$

## Detection of Textures

As the interaction effects are mainly variation due to Cartesian coordinates that results in textures, and main effects are variations resulting in noise, microtextures can be detected based on these local properties. The following two conjectures are proposed in this regard:

**Texture Conjecture 1.** *For a textured region, each interaction mean square does not estimate the same variance.*

**Texture Conjecture 2.** *For a textured region, mean squares corresponding to some members of the set of main effects may estimate the same variance.*

These two conjectures are applied to determine whether the image region under analysis is a textured

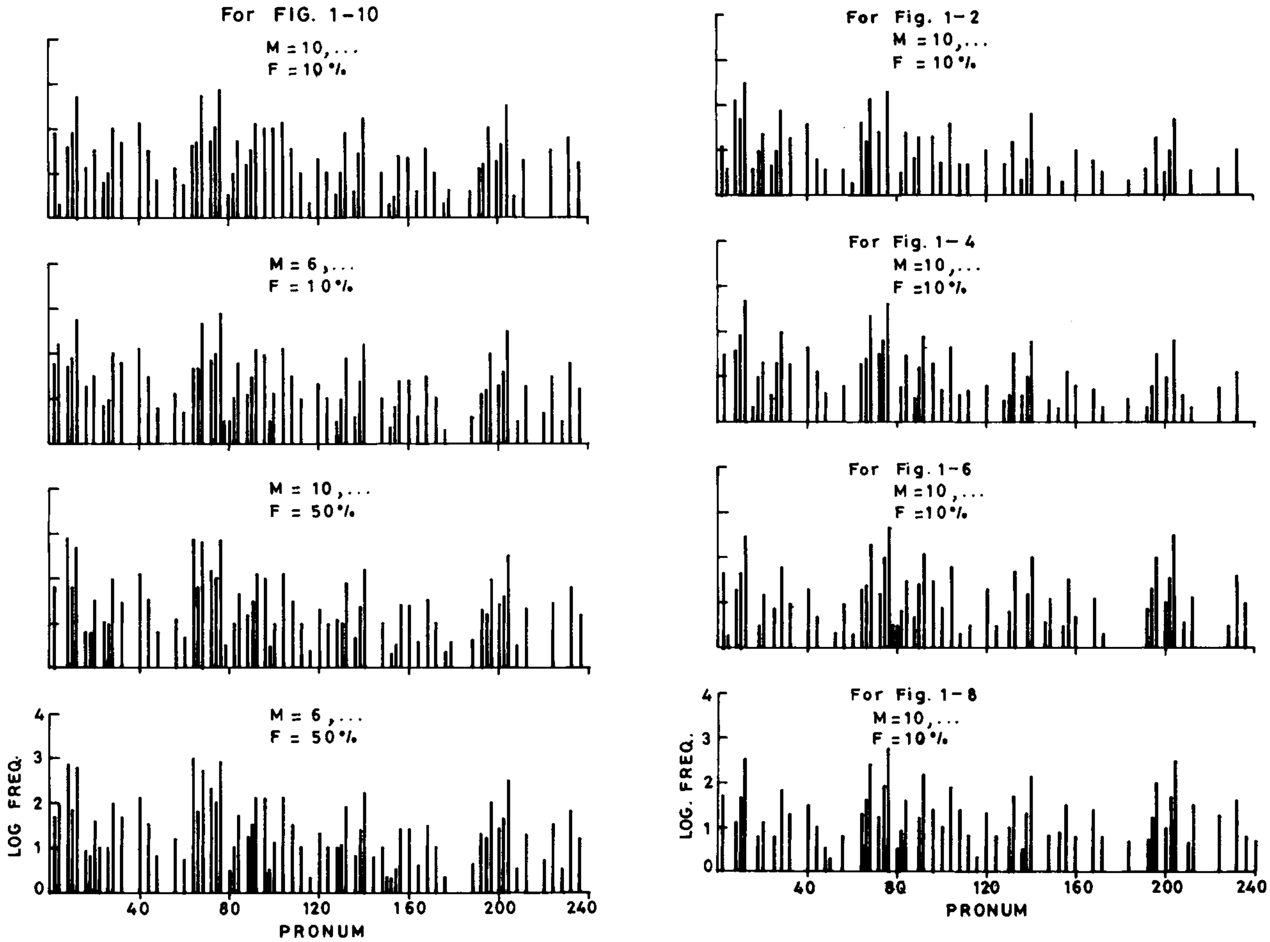


**Figure 3** (a) Prospectrums for the image shown in Figure 1-10 for different significance levels in $M$ and $F$. (b) Prospectrums for the images shown in Figure 1-2, 1-4, 1-6, and 1-8 for the significance levels $M$ = 10, . . . and $F$ = 10%.

region. As each of the mean-square variances corresponding to main and interaction effects is a $\chi^2$ (chi-squared) variate with a degree of freedom of 1, Nair's[11] statistical test (given in Appendix A) toward homogeneity of variances can be applied to check whether mean-square variances corresponding to the main effects are estimates of the same variance and interaction mean squares do not estimate the same variance.

**Table I Statistical Weighted Mean from Figure 1**

| | | "Apparent" Values | | | | | | | "Real" Values | | | | | | |
|---|---|---|---|---|---|---|---|---|---|---|---|---|---|---|---|
| *M* | *F* | 1 | 2 | 3 | 4 | 6 | 8 | 10 | 1 | 2 | 3 | 4 | 6 | 8 | 10 |
| 10, . . | 10% | 4.00 | 4.88 | 4.98 | 5.75 | 9.85 | 11.24 | 14.81 | 0.13 | 0.16 | 0.17 | 0.19 | 0.33 | 0.37 | 0.49 |
| 8, . . | | 4.22 | 5.19 | 5.23 | 6.08 | 10.07 | 11.44 | 14.87 | 0.14 | 0.17 | 0.18 | 0.20 | 0.34 | 0.38 | 0.50 |
| 6, . . | | 5.83 | 7.00 | 7.72 | 8.27 | 12.72 | 14.36 | 17.17 | 0.19 | 0.23 | 0.26 | 0.28 | 0.42 | 0.48 | 0.57 |
| 10, . . | 25% | 4.07 | 4.93 | 5.05 | 5.82 | 10.08 | 11.49 | 15.03 | 0.14 | 0.16 | 0.17 | 0.19 | 0.34 | 0.38 | 0.50 |
| 8, . . | | 4.33 | 5.27 | 5.33 | 6.17 | 10.35 | 11.71 | 15.09 | 0.14 | 0.18 | 0.18 | 0.21 | 0.34 | 0.39 | 0.50 |
| 6, . . | | 6.02 | 7.15 | 7.89 | 8.41 | 13.21 | 14.89 | 17.48 | 0.20 | 0.24 | 0.26 | 0.28 | 0.44 | 0.50 | 0.58 |
| 10, . . | 50% | 4.75 | 5.61 | 5.83 | 6.48 | 12.15 | 13.95 | 17.06 | 0.16 | 0.19 | 0.19 | 0.22 | 0.41 | 0.47 | 0.57 |
| 8, . . | | 5.13 | 6.07 | 6.21 | 6.96 | 12.5 | 14.25 | 17.16 | 0.17 | 0.20 | 0.21 | 0.23 | 0.42 | 0.48 | 0.57 |
| 6, . . | | 7.23 | 8.29 | 9.12 | 9.63 | 15.89 | 18.21 | 19.88 | 0.24 | 0.28 | 0.30 | 0.32 | 0.53 | 0.61 | 0.66 |

### Texture Representation

A small image region [g] of size $(N * N)$ in a digital image is considered as a sample. The two conjectures are applied as per the procedure given in the previous section. Finally, the local descriptor of the texture, pronum, is computed as follows: The mean squares of interaction and main effects are tested for homogeneity of variances.[11] If a sample passes the test, it has to be described properly by suitable representation so that a better local descriptor can be obtained. The following is the procedure:

1. Compute the mean-square error variance (msv) from mean squares of the main effect which are estimates of the same variance.
2. For each member in the set of interaction mean squares and the members which are not included for the computation of msv, perform the $F_{-}$ ratio test.[12]
3. In the $F_{-}$ ratio test, if the $i^{th}$ effect out of $(N^2 - 1)$ effects is significant, the corresponding position has a value of 1; otherwise, it has a value of 0.
4. The small $(N * N)$ image region is represented by a number in the positional number system with radix 2.

The computed number is called pronum. Usually, a $(3 * 3)$ image region is considered as a sample. This image region [g] is represented by eight binary digits $s_i$. Hence,

$$pronum = \sum_{i=1}^{8} s_i * 2^{i-1}, \quad (9)$$

where

$$s_i = \{0, 1\}.$$

The pronum is substituted in the place of the center pixel of the [g]. In the subsequent phase, adjacent regions are considered by sliding a $(3 * 3)$ window and the same procedure is repeated. So, the entire image is mapped into an array of pronums. The range of pronums considered here is (0–255). The frequency of occurrences of these pronums is used as a global descriptor of the texture present in the image. The entire procedure is given in the form of an algorithm in Appendix B.

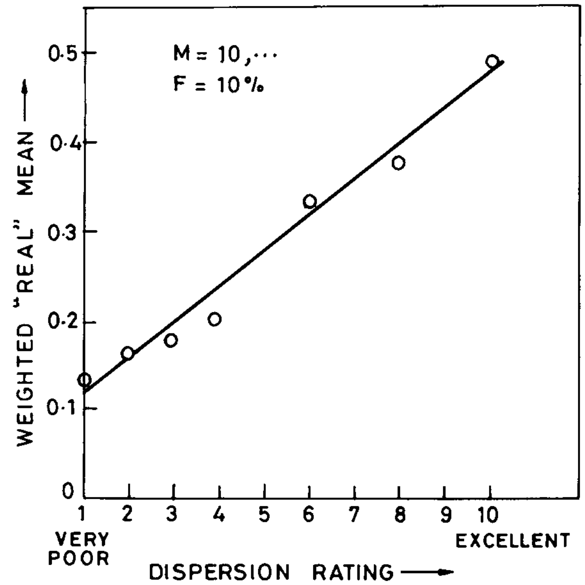


**Figure 4** Plot of weighted "real" mean vs. the dispersion rating.

**Table II Statistical Weighted Variance from Figure 1**

| | | "Apparent" Values | | | | | | | "Real" Values | | | | | | |
|---|---|---|---|---|---|---|---|---|---|---|---|---|---|---|---|
| *M* | *F* | 1 | 2 | 3 | 4 | 6 | 8 | 10 | 1 | 2 | 3 | 4 | 6 | 8 | 10 |
| 10, . . | 10% | 431.5 | 505.2 | 506.2 | 599.3 | 1309.7 | 1493.6 | 1705.5 | 0.48 | 0.56 | 0.56 | 0.67 | 1.45 | 1.66 | 1.89 |
| 8, . . | | 449.9 | 536.8 | 528.1 | 627.7 | 1333.3 | 1514.2 | 1709.2 | 0.50 | 0.60 | 0.59 | 0.70 | 1.48 | 1.68 | 1.90 |
| 6, . . | | 634.6 | 720.7 | 767.6 | 829.4 | 1642.9 | 1863.0 | 1918.8 | 0.70 | 0.80 | 0.85 | 0.92 | 1.82 | 2.07 | 2.13 |
| 10, . . | 25% | 433.5 | 506.2 | 508.1 | 601.5 | 1318.9 | 1502.6 | 1711.8 | 0.48 | 0.56 | 0.56 | 0.67 | 1.47 | 1.67 | 1.90 |
| 8, . . | | 453.3 | 538.2 | 530.8 | 630.5 | 1345.4 | 1523.5 | 1715.7 | 0.50 | 0.60 | 0.59 | 0.70 | 1.49 | 1.69 | 1.90 |
| 6, . . | | 640.6 | 722.9 | 770.9 | 831.5 | 1661.9 | 1881.9 | 1925.9 | 0.71 | 0.80 | 0.86 | 0.92 | 1.85 | 2.09 | 2.14 |
| 10, . . | 50% | 456.0 | 531.1 | 537.4 | 623.9 | 1406.7 | 1602.9 | 1771.2 | 0.51 | 0.59 | 0.59 | 0.69 | 1.56 | 1.78 | 1.97 |
| 8, . . | | 482.0 | 568.4 | 564.6 | 658.7 | 1438.4 | 1631.9 | 1776.3 | 0.54 | 0.63 | 0.63 | 0.73 | 1.59 | 1.81 | 1.97 |
| 6, . . | | 685.2 | 762.4 | 814.6 | 873.9 | 1775.0 | 2032.6 | 1991.9 | 0.76 | 0.85 | 0.91 | 0.97 | 1.97 | 2.26 | 2.21 |

**Table III Fisher Distance Between Texture Plates**

| *M* | *F* | 1-2 | 1-3 | 1-4 | 1-6 | 1-7 | 1-8 | 1-10 |
|---|---|---|---|---|---|---|---|---|
| 10, . . | 10% | 0.02 | 0.02 | 0.04 | 0.10 | 0.13 | 0.12 | 0.17 |
| 8, . . | | 0.02 | 0.02 | 0.04 | 0.10 | 0.13 | 0.12 | 0.17 |
| 6, . . | | 0.02 | 0.03 | 0.04 | 0.10 | 0.12 | 0.13 | 0.16 |
| 10, . . | 25% | 0.02 | 0.02 | 0.04 | 0.10 | 0.13 | 0.13 | 0.18 |
| 8, . . | | 0.02 | 0.02 | 0.04 | 0.11 | 0.13 | 0.12 | 0.17 |
| 6, . . | | 0.02 | 0.03 | 0.04 | 0.12 | 0.11 | 0.13 | 0.16 |
| 10, . . | 50% | 0.02 | 0.02 | 0.04 | 0.12 | 0.13 | 0.14 | 0.19 |
| 8, . . | | 0.02 | 0.02 | 0.04 | 0.12 | 0.11 | 0.15 | 0.18 |
| 6, . . | | 0.02 | 0.03 | 0.04 | 0.12 | 0.12 | 0.13 | 0.18 |
| Avg | | 0.02 | 0.03 | 0.04 | 0.11 | 0.12 | 0.13 | 0.17 |

## EXPERIMENTAL

The photographs which are taken for quantitative analysis are shown in Figure 1. These photographs were supplied by Degussa AG, Germany.[13] These were part of the former Phillips Petroleum Dispersion test for carbon black. Although the formulation generally did not play an important role in making a series of photographs with different dispersion ratings, the recipe which was used for their photographs was as follows: polybutadiene, 30; SBR 1712, 96.25; carbon black N220, 70; oil, 13.75; ZnO, 3; stearic acid, 2; antioxidant, 3; wax, 2; sulfur, 2; and sulfenamide accelerator, 1.3. The photomicrographs showing different dispersion ratings were achieved by adjusting the time of mixing and the speed of rotors in the mixer. The photographs of samples, cut by a special cutter, were taken by a microscope–Poloroid Land Camera combination with an effective magnification of 30×. All the magnified micrographs shown in Figure 1 were digitized in a closed chamber (with uniform illumination) by an electronic scanner (TMC 56 GN-PULNIX CCD camera with a 512 × 512 pixel resolution and focal length of 16 and 8 mm for close and long range) attached to the Benchmark IPS. The digitized version of the representative micrographs of Figure 1-2 and 1-8 is given in Figure 2. Details of the micrographs were provided by Degussa.

## METHOD OF QUANTIFICATION OF DISPERSION

The proposed algorithm was used for analyzing the images with various dispersion ratings shown in Figure 1. The prospectrums were obtained using the procedure described in the previous section. The following parameters were calculated from the prospectrums in order to quantify images based on the textural characteristics present.

### Weighted Mean

Representing the "apparent" weighted mean of the prospectrum by $\mu$, the pronum by $x_i$, and the frequency of occurrence of the pronum $x_i$ by the function $F(x_i)$, the "apparent" weighted mean was computed by

$$\mu = \sum_{i=0}^{255} \frac{F(x_i)}{R \times C} \times x_i \qquad (10)$$

where $R \times C$ is the total number of pixels in the image. (In our case, the image size was 160 × 180.) The numbers obtained were converted into "real" quantities by taking into consideration the actual population and its magnification in the photographs.

### Variance and Standard Deviation

The "apparent" variance ($\sigma^2$) and the standard deviation ($\sigma$) for the prospectrums were obtained as follows:

$$\sigma^2 = \sum_{i=0}^{255} (x_i - \mu)^2 \times \frac{F(x_i)}{R \times C}$$

$$\sigma = \sqrt{(variance)} \qquad (11)$$

The "real" quantities were also calculated by taking into consideration the actual population and its magnification in the photographs.

### Fisher Distance

The statistical distance measured between two textured images in terms of their prospectrums was calculated by the following parameter:

$$\text{Fisher distance} = \frac{|\mu_1 - \mu_2|}{\sigma_1 + \sigma_2} \qquad (12)$$

## RESULTS AND DISCUSSION

The photographs (Fig. 1) show pictures of excellent (9–10), good (7–8), fair (5–6), poor (3–4), and very poor (1–2) dispersion of carbon black fillers in rubber. (The numbers in the parentheses indicate the dispersion rating, as reported by Degussa.[13]) The ratings are, however, based on visual inspection and are arbitrary. These photographs were digitized to a size of 160 × 180 pixels by an electronic scanner attached to the Bench mark IPS. These images have a gray-level variation from 0 to 255. The digitized images of representative photographs of Figure 1-2 and 1-8 are shown in Figure 2. The prospectrums of the representative images (Fig. 1-10, 1-8, 1-6, 1-4, and 1-2) are shown in Figure 3 at various significance levels of $M$ and $F$. Figure 3(a) shows prospectrums of the image (Fig. 1-10) for different significance levels and Figure 3(b) shows the prospectrums of the images (Fig. 1-2, 1-4, 1-6, and 1-8) at $M = 10$, ... and $F = 10\%$ significance levels. The prospectrums have more components and increase in frequency as $M$ and $F$ significance levels are relaxed, i.e., a sample which may not pass the conjecture at the 5% significance level may pass at 10% or higher, leading to increased frequency of occurrence of the pronum. The values of the "apparent" mean and their corresponding "real" mean calculated using eq. (10) are provided in Table I. Similarly, the variances calculated using eq. (11) are reported in Table II. The difference between the "real" and the "apparent" values is due to the magnification of the photographs. The following discussion is based on the "real" values.

The weighted mean of the prospectrum gives directly the number of pronums present in the prospectrum. The total number of pronums present in the prospectrum reveals the amount of textured information present in the image under consideration. The low mean value indicates that the textural information is less or, in other words, that more untextured regions are present. This results from the fact that the carbon blacks are not fully mixed and the dispersion is very poor. As the carbon black particles are dispersed well, the textural information also increases and a higher mean is obtained. The weighted mean values have been calculated for the images shown in Figure 1.

Similarly, the weighted variance is also related to the dispersion rating. For the image shown in Figure 1-1 (very poor dispersion), only a few combinations of pronums are present in the prospectrum, because of poor carbon black mixing. On the other hand, for the image shown in Figure 1-10 (excellent dispersion), large numbers of pronums with different frequencies are present because the carbon blacks are well mixed. The former case, because of the lesser number of pronums, gives low variance, and in the latter case, the variance is higher because almost all pronums are present at different frequencies.

It is interesting to note that as the dispersion is improved the mean value becomes larger. The variance also follows a similar trend at a particular value of $M$ and $F$. For example, the photograph showing a very poor dispersion rating (Fig. 1-1) has a mean value of 0.13. This is much smaller, about one-fourth that of 0.49 determined for a photograph showing an "excellent" dispersion rating (Fig. 1-10). The "mean" values are then plotted against the dispersion rating in Figure 4. It is evident from the plot that, as the dispersion rating goes from very poor to excellent, the "mean" increases proportionately. Also, the values have been compared using the Fisher distance [eq. (12)]. The results are shown in Table III. As the difference between the plates increases, the Fisher distance increases. The values reported in Table III show the difference between plate 1 (Fig. 1-1) (very poor dispersion) and the other plates. It is clear that this distance is almost eight times when the results of $Fd_{1\text{-}2}$ and $Fd_{1\text{-}10}$ are compared. Hence, the present method is not only capable of quantifying dispersion, but is useful in distinguishing between different levels of dispersion (various texture plates).

## CONCLUSIONS

An image-processing technique for characterizing the presence of texture has been applied successfully for quantification of dispersion of carbon black in rubber. The textured surfaces have been represented in terms of a closed set of orthogonal polynomials and the variation in Cartesian coordinates has been measured in terms of main and interaction effects. The main effects are the effects in which one coordinate is varying while the other remains constant, whereas the interaction effects are the effects due to the variation of both coordinates. Conjectures have been proposed for quantifying the texture present. The texture thus identified is described locally by the pronum and globally by the prospectrum. Several statistical parameters are computed from the prospectrum and are correlated with the dispersion rating. The dispersion rating is proportional to the statistical weighted mean obtained from the prospectrum. As the dispersion goes from very poor to excellent, the weighted mean goes from a lower value to a higher value. The statistical closeness between different textured (dispersion rating) surfaces are also measured in terms of the Fisher distance computed between their respective prospectrums. By using this method, the arbitrary conclusions on dispersion can be easily overcome. Furthermore, the classification to which the dispersion rating belongs to can be categorized, which is a real requirement in industry.

The authors are thankful to Degussa AG, Germany, for providing the photomicrographs for this study.

## APPENDIX A: BISHOP AND NAIR TEST

The Nair's test for checking the homogeneity of variances is given below. Let $v_{a_1}, v_{a_2}, \ldots, v_{a_k}$ be the set of variances with $\upsilon_1, \upsilon_2, \ldots, \upsilon_k$ degrees of freedom, respectively. The average variance

$$v_{av} = \frac{1}{\upsilon} \sum_{i=1}^{k} v_{a_i} \upsilon_i$$

and the total degrees of freedom

$$\upsilon = \sum_{i=1}^{k} \upsilon_i$$

Then, the criterion for computing the divergence among variances is

$$M = \upsilon \ln v_{av} - \sum_{i=1}^{k} \upsilon_i \ln(v_{a_i})$$

The values of $M$ for different degrees of freedom for different % of significance levels are given in Ref. 11.

## APPENDIX B: ALGORITHM

**Input** Gray-level image $G$ of size ROW∗COL. [] denotes the matrix and the suffix denotes the elements of the matrix. Let $[M]$ be the polynomial operator and $[f]$ be a $(3 * 3)$ image region extracted from $G$. PROARR holds the pronums obtained from $G$.
**Output** Prospectrum, i.e., frequency of occurrences of pronums (at most 256 different pronums may appear).

**Begin**

**Step 1** Compute $[W] = [M]^t[M]$, where

$$[M] = \begin{bmatrix} 1 & -1 & 1 \\ 1 & 0 & -2 \\ 1 & 1 & 1 \end{bmatrix}$$

**Step 2** Repeat through step 15 for $k = 2$ to ROW-1.
**Step 3** Repeat through step 14 for $l = 2$ to COL-1.
**Step 4** Extract a small region $[f]$ from $G$ centered at $(k, l)$.
**Step 5** Compute $[\beta'] = [M]^t[f][M]$.
**Step 6** Compute $[\beta] = ([M]^t[M])^{-1}([M]^t[f][M]) \times ([M]^t[M])^{-1} = [\beta']/([W]_{i,i} * [W]_{j,j})$.
**Step 7** Compute $[Z] = ([\beta']_{i,j})^2/([W]_{i,i} * [W]_{j,j})$.
**Step 8** $A = \{Z_{01}, Z_{02}, Z_{10}, Z_{20}\}$ are variances due to the main effects and $B = \{Z_{11}, Z_{12}, Z_{21}, Z_{22}\}$ are variances due to the interaction effects.
**Step 9** Perform Nair's test for set $A$ and $B$. If the test fails, pronum $= -1$, indicating that there is no texture. Go to step 14. (While performing Nair's test, if all the four variances do not pass the test, then eliminate one variance at a time and perform the test again. In the worst case, there must be two variances present.)
**Step 10** Let set $V \subseteq A$ has variance terms which pass the Nair's test and $\|V\|$ be the cardinality of set $V$.
**Step 11** Compute the mean square error variance, $msv = (\sum_{Z_{ij} \in V} Z_{ij})/\|V\|$.
**Step 12** Perform the variance ratio test ($F$ ratio test) with the numerator as one of the variances from $\{A + B - V\}$ and msv as the denominator against the chosen significance level. If the test is significant, the corresponding position $p_i$ of the numerator in the image region $[f]$ is marked as 1, else as 0.

**Step 13** Compute the pronum for the image region [$f$] as, $pronum = \sum_{i=1}^{8} p_i * 2^{i-1}$, $p_i = 1$ if the $i^{th}$ position is 1; otherwise 0.
**Step 14** Store the pronum in PROARR[$k$][$l$] and increment $l$ by 1.
**Step 15** Increment $k$ by 1.
**Step 16** Compute the frequency of occurrences of pronums from PROARR.
**End**

## REFERENCES


1. W. M. Hess, *Rubber Chem. Technol.,* **64,** 386 (1991).
2. A. I. Medalia, *Rubber Age,* **97,** 82 (1965).
3. W. M. Hess and G. C. McDonald, *Rubber Chem. Technol.,* **56,** 892 (1983).
4. P. Shih and G. C. Goldfinger, *Rubber World,* **199,** 31 (1989).
5. R. Kadunce, *Rubber Chem. Technol.,* **47,** 469 (1974).
6. L. Ganesan and P. Bhattacharyya, *Pattern Recognition,* **28,** 1 (1995).
7. R. M. Haralick, *Proc. IEEE,* **67,** 786 (1979).
8. M. M. Galloway, *Computer Graphics and Image Processing,* **4,** 172 (1975).
9. D. C. He and L. Wang, *IEEE Trans. Geo Sci. Remote Sensing,* **28,** 509 (1990).
10. P. Bhattacharyya, PhD Thesis, Dept. of Computer Science and Engineering, IIT, Kharagpur, 1984.
11. D. J. Bishop and U.S. Nair, *Biometrika,* **30,** 89 (1939).
12. R. A. Fisher and F. Yates, *Statistical Tables for Biological, Agricultural and Medical Research,* Oliver and Boyd, London, 1947.
13. E. A. Booth, J. C. Bouguin, and M. Haddeman, Degussa AG, Germany, Private communication, 1994.


*Received July 12, 1994*
*Accepted November 2, 1994*